ISSN: 2977-0041

Research Article

Journal of Material Sciences and Engineering Technology

Structural, Dielectric and AC Conductivity of Gadolinium Modified $Bi_{0.4}Na_{0.4}Sr_{0.2}TiO_3$ Composite

Venkata Yamini Kanth Kara[1], Sharma NK[2], Ahamad Mohiddon MD[1] and Anshu Gaur[1*]

[1]*Center for Nanoscience and Nanotechnology, Department of Physics, Faculty of Science and Humanities, SRM University Delhi-NCR, Sonepat, 131029, Haryana*

[2]*Department of Mechanical Engineering, Faculty of Engineering, SRM University Delhi-NCR, Sonepat, 131029, Haryana, India*

[*]**Corresponding author**

Anshu Gaur, Center for Nanoscience and Nanotechnology, Department of Physics, Faculty of Science and Humanities, SRM University Delhi-NCR, Sonepat, 131029, Haryana, India.

Received: July 21, 2025; **Accepted:** July 29, 2025; **Published:** August 06, 2025

ABSTRACT

This work investigates structural and dielectric-electrical properties of Gd-modified $Bi_{0.5}N_{0.5}TiO_3$, i.e. $(Bi_{0.34}Gd_{0.06})$ $Na_{0.4}Sr_{0.2}TiO_3$ (BNSGT) ceramic. X-ray diffraction technique is used to confirm the crystal structure and associated properties such as crystallite size and lattice strain. The crystallite size was estimated from the refined peak width using Halder-Wagner and Debye-Scherrer's equations to highlight the presence of lattice strain, which is crucial for ferroelectric polarization. The dielectric characteristics of BNSGT are recorded as a function of temperature and frequency to unveil the nature (thermal) and dynamics of various processes, such as dipolar and charge conduction. The structural analysis suggested the shift of the crystal structure towards asymmetry, which is beneficial for enhancing the ferroelectric polarization, whereas dielectric data analysis by Cuire-Weiss law, relaxation peak indicated good polarization attributes while maintaining a lower dielectric loss, less than 0.05. The results highlight the potential of Gd-modified BNST composites for advanced applications in solid-state cooling technologies.

Keywords: Dielectric-Electrical, Gadolinium, Electrocaloric, Rhombohedral

Introduction

Refrigeration based on electrocaloric effect (ECE) is strikingly attractive as it promises environment-friendly cooling at higher efficiency (70%) compared to (unhealthy) vapor compression-based refrigeration (50%). The electrocaloric effect, characterized by a reversible temperature change in a material under an applied electric field, has emerged as a promising route for developing sustainable cooling technologies. Ferroelectric materials, with their ability to exhibit spontaneous polarization reversible by an external electric field, are at the forefront of ECE research due to their potential for high electrocaloric performance [1]. Among these, perovskite-based ceramics, such as $Bi_{0.5}Na_{0.5}TiO_3$ (BNT), have garnered significant attention for their lead-free composition, high polarization, and tunable dielectric properties, making them ideal candidates for next-generation cooling devices, sensors, and actuators [2-4]. The $Bi_{0.5}Na_{0.5}TiO_3$ based system, particularly when modified with strontium (Sr) to form $Bi_{0.4}Na_{0.4}Sr_{0.2}TiO_3$ (BNST), offers a robust platform for tailoring structural and electrical properties. The incorporation of Sr at the A-site of the perovskite structure enhances phase stability and dielectric response, making BNST a versatile material for multifunctional applications. However, to further optimize its electrocaloric and dielectric performance, doping with rare-earth elements, such as gadolinium (Gd), is a promising strategy. Gadolinium, with its unique ionic radius and electronic configuration, can influence the crystal structure, polarization dynamics, and dielectric behavior, potentially enhancing the electrocaloric effect and AC conductivity.

In this study, we examine the structural, dielectric, and AC conductivity properties of gadolinium-modified $Bi_{0.4}Na_{0.4}Sr_{0.2}TiO_3$ composites. By systematically doping Gd into the BNST matrix, we aim to elucidate the role of rare-earth substitution on phase formation, dielectric tunability, and charge transport mechanisms. The structural characteristics of

Citation: Venkata Yamini Kanth Kara, Sharma NK, Ahamad Mohiddon MD, Anshu Gaur. Structural, Dielectric and AC Conductivity of Gadolinium Modified $Bi_{0.4}Na_{0.4}Sr_{0.2}TiO_3$ Composite. J Mat Sci Eng Technol. 2025. 3(3): 1-4. DOI: doi.org/10.61440/JMSET.2025.v3.63

the composition are analyzed using X-ray diffractometer and scanning electron microscopy (SEM) while dielectric properties and AC conductivity are evaluated across a range of frequencies and temperatures. These insights are critical for understanding the interplay between structural modifications and electrical performance, paving the way for the development of high-efficiency electrocaloric materials for sustainable refrigeration technologies.

Materials and Methods

Gd-doped $Bi_{0.4}Na_{0.4}Sr_{0.2}TiO_3$ is synthesised by the Solid-state mixed oxide method. Stoichiometrically weighed constituent oxides and carbonates are wet mixed homogeneously using an agate mortar and calcined in a muffle furnace at 900°C for 12 h. The powders are pelletized by applying a pressure of approximately 1 GPa using a hydraulic press and sintered at 1250°C for 2 h. Crystal structure characterization of the composition is performed using an X-ray diffractometer (Malvern's PANalytical X'pert Pro). The crystal diffraction data is recorded in the 2θ range of 20° to 70° using Cu k_α radiation (λ = 1.5406Å). Dielectric characterization of the Gd-modified BNST was performed using an impedance analyzer (nF LCR meter, Model ZM2376) across a range of frequencies (20 Hz 2 MHz) and temperatures (30°C – 300°C). Before the dielectric measurement, the pellet was polished with a final diameter of ~9.7 mm and a thickness of ~ 1 mm. The pellet was converted to a capacitor-like structure by applying silver paste on both of the circular faces and dried in a hot air oven for an hour.

Results and Discussion

Figure 1 shows the X-ray diffraction spectra of Gd-modified BNST. The diffractograph consists of a set of seven peaks, with the most intense one lying at 2θ = 32.49°. No more peaks are present within the detection limit of the diffractometer, indicating that the generated sample is a single phase. These peaks are associated with the rhombohedral crystal structure of space group R3c, as listed in the JCPDS file number 98-029-1528. The structural identification is confirmed by refining the data using FullProf software. The refinement provided a goodness of fit of 16 and R_{wp} of 6.3 and an intensity difference between the experimental and generated data of the most intense peak of less than 10%. These values indicate a stable fit or representation of the experimental data. The hexagonal lattice parameters thus obtained are $a = b =$ 5.487 Å and c 13.437 Å against $a = b =$ 5.511 Å and $a = b =$ 13.491 Å of pure BNST. The rhombohedral lattice parameters (a_R and α_R) are calculated from the hexagonal to rhombohedral conversion formula: $\alpha_R = \frac{1}{3}\sqrt{(3a^2 + c^2)}$ and $(\alpha_R/2) = \frac{3}{2\sqrt{(3+(c/a)^2)}}$ and are obtained to be 5.486 Å and 60.041o, respectively, against a_R 5.509 Å and α_R 60.057o of pure BNST. The incorporation of a smaller Gd3+ ion is reflected in the decreased unit cell parameters of BNST that also causes the rhombohedral cell to be more asymmetric (i.e. away from cubic for which α = 90°). With the refined crystal structure parameters, the unit cell is visualized using Vesta software and shown in Figure 1(c).

From the refined peak positions, crystallite size (D) and lattice strain (ε) are calculated using the Halder-Wagner method, which is mathematically expressed as,

$$\left(\frac{\beta}{\tan\theta}\right)^2 = \frac{k\lambda}{D}\left(\frac{\beta}{\tan\theta\sin\theta}\right) + 16\varepsilon^2$$

where β is the full width as half maximum of X-ray diffraction peak position at 2θ,θ being the Bragg angle and k is a shape factor, generally taken to be 0.9. H-W method takes into account that the peak broadening due to crystallite size and lattice strain is convoluted. Scherrer's method or equation does not consider the presence of lattice strain. To strongly claim the presence of lattice strain, both methods are employed to calculate the D. The D value from the H-W method is 54 nm, whereas that from Scherrer's method for the most intense peak is 38 nm. Such a difference is defensible by the presence of a lattice strain of 1.81 x 10^{-3}. Also, such a significant strain value is typical of ferroelectric materials [5].

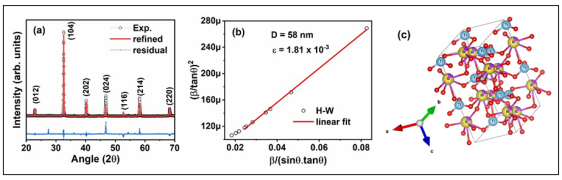

Figure 1 (a): Experimental and Rietveld method refined/ generated X-ray diffraction data of Gd modified BNST, (b) H-W method employed for the calculation of crystallite size and lattice strain and (c) atomic arrangements of Gd doped BNST obtained using Vesta software

Dielectric constant (∈') and dielectric loss (tanδ) of Gd modified BNST are shown in Figure 2a and 2b. ∈'(T) of BNSGT is characterized by multiple peaks, which is typical of bismuth sodium titanate [Sakata, Ranjeet et al]. The ferroelectric to antiferroelectric phase transition temperature in Gd-modified composition is observed at 124°C. This transition in pure BNT is reported to occur at approximately 210°C, whereas it is reduced to 110°C for 20% and to approximately room temperature for 25% Sr-doped BNT [6,7]. The increment in TC by 6% Gd substitution in 30% Sr-doped BNST is correlated with the change in the crystal structure. Ferroelectricity is the attribute of an asymmetric crystal structure, lacking center of symmetry. The stability of perovskites in different geometries is understood in terms of the Goldschmidt tolerance factor, which is given as, $t = (r_A + r_0)/\sqrt{2}(r_B + r_0)$ with r_A, r_o and r_B are the ionic radii of A-site, B-site cations and Oxygen ions. t = 1 represents the most symmetric cubic structure, whereas t between 0.71 – 0.9 is for rhombohedral arrangement. In BNST, the effective ionic radius of A-site cation is calculated as the average of Bi^{3+}, Na^+ and Sr^{2+} ions and is observed to be 1.0715, which leads to t of 0.7734. The substitution of Gd (rGd^{3+} = 93.5 pm) for Bi (rBi^{3+} = 103 pm) decreases the effective ionic radius of the A-site cations to 1.0660 pm pm and t to 0.7717. This modification causes t to shift away from 1 and makes the crystal a little more asymmetric which may contribute to the overall polarization and ferroelectricity.

The ferroelectric behaviour of BNSGT can be further characterized/ quantified using the Curie-Weiss law, mathematically given as, ∈ = $C/(T\text{-}T_C)$ where C is Curie constant and is directly proportional to the dipole concentration and effective dipole moments and T_C represents the temperature below which the material becomes ferroelectric. A graph is plotted between 1/eps and T. In the temperature region higher than 320°C, the graph shows a linear dependence, indicating the validity of the Curie-Weiss law. From the slope and the intercept, the constants C and T_C are observed to be 1.2 x 10^5 K and 145 K at 20 kHz. The C value is typical of

ferroelectric materials [5,8]. Further, the dielectric loss is in the range of 0.02-0.055 at RT-125°C at all the measured frequencies, indicating good ferroelectric or charge storage behaviour of the BNST.

To further characterize the dielectric properties and investigate the dielectric loss mechanism, AC conductivity is calculated using the relation $\sigma = \omega\epsilon_0 \epsilon''$. To discern the processes that are thermally activated and follow the Arrhenius relation $\sigma = \sigma_0 e^{-E_a/kT}$, a graph between *ln* σ and $10^3/T$ is plotted. It can be seen in Figure 2(c) that the dependence is linear in the temperature range of 310°C- 360°C wherein BNSGT is paraelectric. It is therefore inferred that at these temperatures, the dominant loss mechanism is charge conduction. From the slope and intercept of the linear portion of the graph, activation energy and the material's constant σ_0 are calculated and shown in Table 1. It can be seen that E_a and σ_0 are strongly frequency-dependent. E_a varies from 0.95 eV at 200 Hz to 0.28 eV at 2 MHz, whereas σ_0 changes from 1.0 x10^{-3} at 200 Hz to 1.6 x 10^{-7} at 2 MHz. Such frequency dependence is in line with the prediction of the charge conduction.

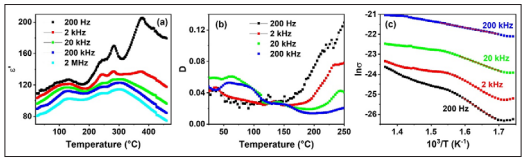

Figure 2: (a) Dielectric constant and (b) dielectric loss as a function of temperature, and (c) Arrhenius plot of AC conductivity.

Table 1: Showing parameters obtained from Curie-Weiss law and Arrhenius relation

S. No.	Frequency	T_C (K)	C x 10^{-5} (K)	E_a (eV)	σ_0 (S/cm)
1	200 Hz	-	-	0.95	1.0 x 10^{-3}
2	2 kHz	-	-	0.85	3.9 x 10^{-4}
3	20 kHz	144	1.18	0.55	4.4 x 10^{-6}
4	200 kHz	296	0.76	0.29	1.6 x 10^{-7}
5	2 MHz	368	0.56	-	-

The dynamic aspect of the dipoles and conduction charges is analyzed using frequency-dependent dielectric constants. Real and imaginary parts of the dielectric constants are shown as a function of frequency, recorded at the constant temperatures of 30°C, 50°C, 100°C, 150°C and similar temperatures up to 500°C, depicted in Figure 3. On observing ϵ'-data at different temperatures, it is noticed that ϵ' (e.g. at 1 MHz) shows an increasing trend up to 150°C, and then it starts decreasing. This trend is similar to that recorded in a temperature sweep measurement, assuring the reliability of the data (and repeatability of the measurement). ϵ' (ω)-ϵ'' (ω) exhibit a characteristic/typical behavior of diminishing with rising frequency. This behavior accounts for only a specific type of dipoles i.e. ferroelectric or orientational dipoles (in addition to ionic and electronic) can respond to megahertz frequency signals. The space charge polarization, which is based on the movement of conduction charges (mainly ions and defects) is unable to follow the rapid electric field variations. The conjugate parameter ϵ'' also shows a similar trend, except for a relaxation behaviour visible for 30°C-150°C temperatures via a peak in the MHz frequency values. At higher temperatures, the peaks possibly shifted to even higher frequencies, beyond the range of used setup. The relaxation time (τ) of the dipoles is estimated from the peak position (ω) in ϵ'' (ω) graph which satisfies the relation ωτ = 1. τ is of the order of 1 x 10^{-7} s which is typical of ferroelectric dipoles [9].

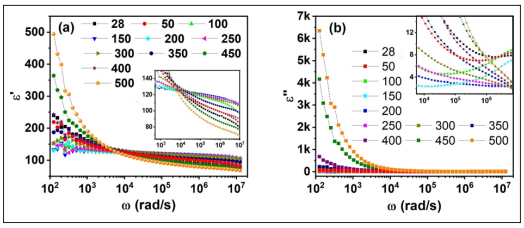

Figure 3: (a) Real and (b) imaginary part of dielectric constant.

Conclusion

6% Gd-doped $Bi_{0.4}Na_{0.4}Sr_{0.4}TiO_3$ is synthesized in a single phase by the solid-state reaction route at 900°C. X-ray diffraction data of the sintered pellet indicate a crystalline phase with rhombohedral crystal structure and that smaller Gd^{3+} doping at Bi^{3+} -site modifies the lattice parameters, *a* and *c*, such that the unit cell becomes more asymmetric. The XRD data were analyzed through Rietveld refinement using FullProf software and the refined peak width was utilized to estimate the crystallite size of 58 nm and lattice strain of 1.81 x 10^{-3} using the Halder-Wagner method. The crystallite size calculated using Scherrer's equation provided a smaller value, supporting the presence of lattice strain.

Gd-doped BNST is characterized by a ferroelectric to antiferroelectric transition around 124°C and a low dielectric loss, approximately 0.05 at temperatures below 150°C, revelaed in delectric characterization. AC conductivity at the temperatures of 310°C-360°C (paraelectric regime) follows the Arrhenius relation and the activation energy of the process was strongly frequency-dependent, for being conduction-related. Frequency-dependent dielectric parameters (ϵ', ϵ'' and σ_{AC}), also indicated, the presence of dipolar and conduction processes, each dominant in different frequency and temperature ranges. The ferroelectric dipoles are characterized by a relaxation time of ~1 x 10^{-7} s. The results highlight the potential of Gd-modified BNST composites for advanced applications in solid-state cooling technologies.

References

1. Valant M. Electrocaloric materials for future solid-state refrigeration technologies, Prog Mater Sci. 2012. 57: 980-1009.
2. Liu X, Zhao Y, Shi J, Du H, Xu X, et al. Improvement of dielectric and ferroelectric properties in bismuth sodium titanate based relaxors through Bi non-stoichiometry, J Alloys Compd. 2019. 799: 231-238.
3. Yang F, Li M, Li L, Wu P, Pradal-Velázquez E, et al. Defect chemistry and electrical properties of sodium bismuth titanate perovskite, J Mater Chem A Mater. 2018. 6: 5243-5254.
4. Schütz D, Deluca M, Krauss W, Feteira A, Jackson T, et al. Lone-pair-induced covalency as the cause of temperature- and field-induced instabilities in bismuth sodium titanate, Adv Funct Mater. 2012. 22: 2285-2294.

5. Gaur A, Dulgaj S, Parida SR, Srinath S. Dielectric and electrocaloric properties of BCTZ composite with cobalt zinc ferrite nanoparticles, Mater Res Bull. 2024. 173: 112639.
6. Sakata K, Masuda Y. Ferroelectric and Antiferroelectric Properties of (Na0.5 Bi0.5) TiO3-SrTiO3 Solid Solution Ceramics, Ferroelectrics. 1974. 7: 347-349.
7. Watanabe Y, Hiruma Y, Nagata H, Takenaka T. Phase transition temperatures and electrical properties of divalent ions (Ca2+, Sr2+ and Ba2+) substituted (Bi1/2Na1/2) TiO3 ceramics, Ceram Int. 2008. 34: 761-764.
8. Ughade RS, Gaur A, Preeti, Rout J, Yadav KL, et al. Ba-Modified Bi–Na–Sr Titanate: Exploring Structural, Dielectric, and Electrocaloric Properties for Cooling Applications. Energy Technology. 2025. 11: 2402094.
9. Van Hong L, Van Khien N, Van Chuong T. Dielectric Relaxation of Ba11xCaxTiO3 (x = 0.0?0.3), Mater Trans. 2015. 56: 1374-1377.

Copyright: © 2025 Anshu Gaur, et al. This is an open-access article distributed under the terms of the Creative Commons Attribution License, which permits unrestricted use, distribution, and reproduction in any medium, provided the original author and source are credited.